Journal of
Polymer & Composites

ISSN: 2321-2810 (Online)
ISSN: 2321-8525 (Print)
Volume 13, Special Issue 5, 2025
DOI (Journal): 10.37591/JoPC

https://journals.stmjournals.com/jopc

Research JoPC

Defect Diagnosis and Modelling for A Rotating Machine Running at A Steady Pace

Rajeev Kumar[1,*], Ravi Kant Singh[2], Ravi Shankar Rai[3], Vikas Kumar[4], Rakesh Dubey[5], Subhash Gautam[6]

Abstract

Rotary equipment, such as gears, shafts, pumps, and bearings, are widely used across various rotary machine in industries, often operating under different loading conditions. The fluctuations in loading can lead to fatigue failures in rotating components, significantly affecting machinery performance. To investigate the behavior of such rotating equipment under diverse operational scenarios, a numerical model has been created. This approach can replace costly and often challenging experimental methods. However, it is essential that the model accurately reflects experimental results. The model's complexity will vary based on the intended purpose of the simulation data. This paper presents dynamic models of a rolling contact ball bearing system and a single-stage spur gear transmission system. These models were created using ADAMS software, which simulates movement in multi-body systems. Both models are scalable, allowing for the introduction of any type of fault. In this study, the models are simulated under constant speed and constant load conditions, and the vibration response of the inner race, outer race, and ball in the case of the rolling contact ball bearing model, as well as the pinion and gear in the case of the gear dynamic model, are captured as vibrational signals. After that, the generated vibration signal is post-processed in MATLAB to evaluate the rotary machine's condition, offering insights into its performance and potential issues. It is analyzed in both time and frequency domains to determine the machine's overall state.

Keywords: Modelling, simulation, gear, bearing, time domain, Frequency domain

INTRODUCTION

In rotary machines, parts like gears, bearings, and shafts can fail unexpectedly. This can happen because of problems like defects in the materials, mistakes during production, too much load, poor installation, or not enough lubrication These failures can lead to significant issues, including unavailability of machines, breakdown time of machines, reduced customer satisfaction, and worker safety risks. To prevent such problems, accurate performance assessments must be conducted by monitoring and classifying the system's health state over time. Since gears and bearings are critical to equipment performance, their condition directly impacts overall machinery efficiency. As a result, researchers have focused on fault diagnosis using vibration analysis, which is crucial for reducing economy losses and minimizing the risk of employee injuries.

Gears and bearings are essential components in several rotary machinery, making fault diagnosis of these systems a crucial area of research [1-3]. Among the various techniques for fault detection, vibration analysis is the most comm only used due to its simplicity in measurement [4-6]. The

***Author for Correspondence**
Rajeev Kumar

[1,2,5,6]Assistant Professor, Department of Mechanical Engineering, Sandip Institute of Technology and Research Centre, Nashik, Maharashtra, India
[3,4]Assistant Professor, Department of Automation and Robotics Engineering, Sandip Institute of Technology and Research Center, Nashik, Maharashtra, India

Received Date: January 16, 2025
Accepted Date: March 22, 2025
Published Date: July 18, 2025

Citation: Rajeev Kumar, Ravi Kant Singh, Ravi Shankar Rai, Vikas Kumar, Rakesh Dubey, Subhash Gautam. Defect Diagnosis and Modelling for A Rotating Machine Running at A Steady Pace. Journal of Polymer & Composites. 2025; 13(Special Issue 5): S154–S164p.

measured vibration signals are analyzed in Time domain [7], frequency domain [8], and time-frequency domain [9–11] to identify the health of rotary machine. The time-frequency technique is widely accepted due to its ability to capture energy spreading in the time-frequency plane.

McFadden et al. [4] introduced a dynamic model of a bearing having an inner race fault at a single point, considering factors such as shaft speed, load distribution on bearings, and vibration decay. The comparison between measured and predicted vibration spectra confirmed the accuracy of their model. Mishra et al. [5] proposed a three deep groove ball bearing model, which varied in complexity and simulation tools (MATLAB Simulink, SYMBOLS, ADAMS). They compared the frequency characteristics of experimental and simulated vibrations for various bearing faults. Guo et al. [6] proposed a vibration separation technique for detecting confined tooth faults in planetary gear sets, addressing the challenge posed by time-varying vibration transfer paths in these systems.

Kumar et al. [12-16] conducted comprehensive studies on gear systems, highlighting the importance of regular gear condition monitoring to detect faults and prevent machine damage, as faulty gear trains exhibit increased vibration amplitudes. Their research includes dynamic models for bevel gear systems, such as an 8-DOF model and a multibody model, to assess system health, develop fault diagnostic tools, and improve system performance [13]. They also examined spur gear systems, revealing that faulty pinions elevate the total vibration magnitude spectrum, underscoring the value of model-based diagnosis for design optimization and maintenance [14]. Furthermore, Kumar et al. [15] modeled a CAD-based epi-cyclic gear train with defects in the sun gear, using MBS ADAMS simulations to demonstrate increased disturbances in faulty systems. Additionally, they employed a 9-DOF kinematics model to analyze gear behavior in both healthy and faulty states, focusing on spur gears with higher contact ratios and solving the equations with Matlab-Simulink [16]. These studies collectively emphasize the critical role of fault detection and system performance enhancement in gear systems. Ozguven and Houser [17] presented a numerical model explaining the dynamics of the gear model. Research studies [18-21] have focused on gear meshing frequencies and the variations in gear meshing stiffness under different fault conditions. The contact force and friction/traction forces are determined using Hertzian contact theory [22]. This paper aims to develop a dynamic model of rolling contact ball bearings and spur gear systems using ADAMS software, analyzing their dynamic response under constant speed operation. The vibration signal characteristics obtained from the simulated model are then studied for fault diagnosis of the system.

Some assumptions considered in ball bearings are as follows:

a. The inner race rotates at a constant speed, while the outer race remains stationary.
b. There is no slipping between balls and races.
c. A massless cage maintains a constant angular separation between the balls around the shaft.
d. The mass of the balls is negligible compared to the other components of the system due to their small size
e. All rotational motions occur around the z-axis, while translational motions take place in the x-y plane.

Figure 1 shows a simplified model of a rolling contact ball bearing with a shaft-connected rotor moving at a constant speed.

The rotational frequency of connector shaft (f_s) is given by

$$f_s = \frac{\omega_s}{2\pi} \qquad (1)$$

The inner race of bearings is anchored to the connector shaft, and the outer race of bearings is supported on flexible supports. As the contact between the ball and races is a point contact, the contact angle is taken as zero degrees. The parameters of the rolling contact ball bearing are shown in Table. 1.

Journal of Polymer & Composites
Volume 13, Special Issue 5
ISSN: 2321-2810 (Online), ISSN: 2321-8525 (Print)

Table 1. Parameters of rolling contact ball bearings.

Parameters	**Value**
Ball diameter (d)	0.794 cm
Inner race diameter	3.158 cm
Outer race diameter	6 cm
Pitch diameter (D)	3.932 cm
Length of inner and outer races, cage	2 cm
Number of balls	9

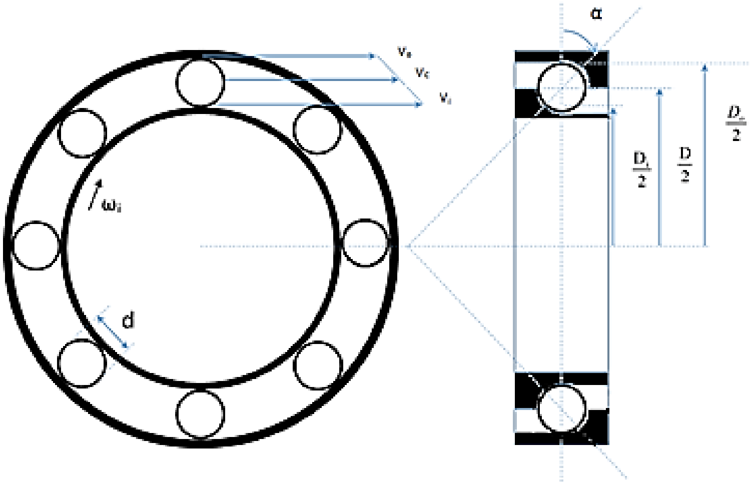

Figure 1. Diagrammatic representation of rolling contact bearing.

where d, D_i, D_o, D, and α denotes the dia. of ball, inner race, outer race, Pitch circle and Contact angle respectively.

From the geometry, the bearing pitch circle diameter can be calculated as:

$$D = \frac{D_i + D_o}{2} \tag{2}$$

The dia. of inner and outer races can be calculated as:

$$D_i = D - d(\cos\alpha) \tag{3}$$

$$D_o = D + d(\cos\alpha) \tag{4}$$

Assuming pure rolling conditions, the circumferential velocities of inner and outer race are as:

$$V_i = \omega_i \times \frac{D_i}{2} \tag{5}$$

$$V_o = \omega_o \times \frac{D_o}{2} \tag{6}$$

Under no slip conditions, the cage velocity is equal to the average velocity of inner and outer race:

$$V_c = \frac{V_i + V_o}{2} \tag{7}$$

Substituting the eqs. (3), (4), (5) and (6) in eqs. (7) becomes

$$V_c = \frac{\omega_i(D - d\cos\alpha)}{4} + \frac{\omega_o(D + d\cos\alpha)}{4} \tag{8}$$

The circumferential velocity in m/sec of rotating elements can be converted into frequency in rev/sec (Hz) by dividing the velocity by πD. The rotational frequency of the cage, also called the fundamental train frequency, is given by

$$f_c = \frac{f_i(1-\frac{d}{D}\cos\alpha)}{2} + \frac{f_o(1+\frac{d}{D}\cos\alpha)}{2} \quad (9)$$

As outer race is considered as fixed, the eqs. (9) is simplified to

$$f_c = \frac{f_i(1-\frac{d}{D}\cos\alpha)}{2} \quad (10)$$

The balls frequency of rotation with respect to inner race is given by

$$\mathrm{f_{bi}} = \mathrm{f_c} - \mathrm{f_i} \quad (11)$$

Substituting eqs. (9) it becomes

$$f_{bi} = \frac{f_o(1+\frac{d}{D}\cos\alpha)}{2} - \frac{f_i(1+\frac{d}{D}\cos\alpha)}{2} \quad (12)$$

For z number of balls, the inner race's ball pass frequency is:

$$f_{bpfi} = \frac{z(f_o-f_i)(1+\frac{d}{D}\cos\alpha)}{2} \quad (13)$$

The balls frequency of rotation with respect to outer race is given by

$$\mathrm{f_{bo}} = \mathrm{f_o} - \mathrm{f_c} \quad (14)$$

Substituting equation (9) it becomes

$$f_{bo} = \frac{f_o(1-\frac{d}{D}\cos\alpha)}{2} - \frac{f_i(1-\frac{d}{D}\cos\alpha)}{2} \quad (15)$$

For z number of balls, the outer race's ball pass frequency is:

$$f_{bpfo} = \frac{z(f_o-f_i)(1-\frac{d}{D}\cos\alpha)}{2} \quad (16)$$

The balls frequency of rotation about their own axes is called as Ball spin frequency. It can be obtained as:

$$f_{bsf} = f_{bi} \times \frac{D_i}{d} \quad (17)$$

Substituting equation (2) and (12) it becomes

$$f_{bsf} = \frac{f_o-f_i}{2}\frac{D}{d}\left(1-\left(\frac{d}{D}\cos\alpha\right)^2\right) \quad (18)$$

Equations (10), (13), (16), and (18) represent the defect characteristic frequencies (DCFs) of the ball bearing with the outer race stationary. These can be used for fault detection in bearings. For the developed model using the parameters in Table. 1, the corresponding DCFs are calculated. See Table. 2.

Table. 2. Characteristic frequencies of developed rolling contact ball bearing model.

Frequency	Value (Hz)
Rotational frequency of Connector shaft (f_s)	10
Fundamental train frequency (f_c)	$0.399 \times f_s$
Ball spin frequency (f_{bsf})	$2.3751 \times f_s$
Ball pass frequency on outer race (f_{bpfo})	$5.4086 \times f_s$
Ball pass frequency on inner race (f_{bpfi})	$3.5913 \times f_s$

Journal of Polymer & Composites
Volume 13, Special Issue 5
ISSN: 2321-2810 (Online), ISSN: 2321-8525 (Print)

MODELLING

Dynamic Modelling of Rolling Contact Ball Bearing System

The rolling contact ball bearing dynamic model, modelled in Adams view, is diagrammatically represented in Figure 2. The model contains a rotor that is rigid in both torsion and bending. It is connected to a motor shaft by a flexible coupling designed by attaching a bushing between them at one end, which provides significant torsional stiffness. This coupling facilitates to accommodate parallel and angular shaft misalignment, as it offers low bending stiffness. The rotor is coupled with a connecting shaft that is seated on two rolling contact ball bearings. The bearings are placed on the pedestals with two spring dampers in the x & y directions to provide stiffness and damping to the bearing mounts. A fixed joint constraint is attached between the inner race of the bearings and the connector, which means the inner races of the bearings move along with the connecting shaft.

A loader is attached to the connecting shaft's far end from the motor to convey radial load on the system. The loader movement is constrained to the connecting shaft by using a fixed joint between them. A bushing having high damping and stiffness in 3 mutually perpendicular directions is attached between the outer races of the bearings and pedestal to withstand the moments and axial forces acting upon the outer race. The balls are modelled as inflexible objects that are contained within a floating body called a cage. The cage doesn't contact either of the outer race or inner race of the bearings. It helps to accommodate the balls at constant angular spacing. Contact forces are defined between the contacting surfaces, viz., between every ball and the outer and inner races, and between the balls and the cage, which will permit a small clearance between the cage grooves and the ball. The calculation of contact force parameters is shown in the next section. The parameters used in the modelling of ball bearings are mentioned in Table. 1.

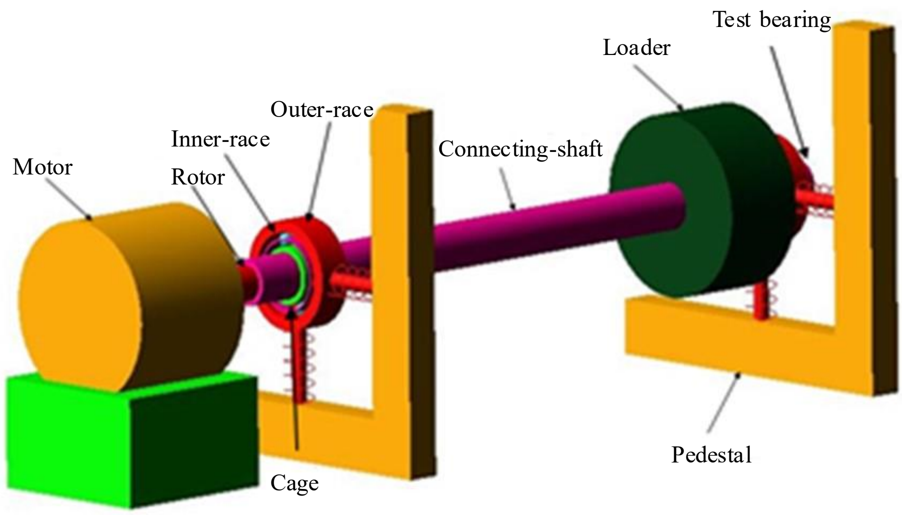

Figure 2. Dynamic rolling contact ball bearing model.

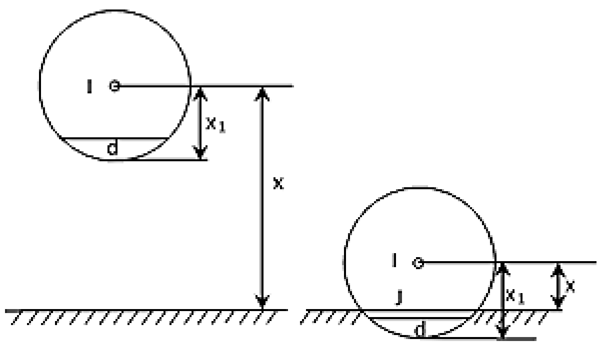

Figure 3. Describing solid to solid contact model in ADAMS [5].

Modelling of contact force between two objects is of two types. One is discontinuous contact, like a bouncing ball on the floor, and the other is continuous contact, defined as a nonlinear spring. For the discontinuous contact, the collision force is calculated by the restitution method. Whereas the impact method is used for continuous contact, which uses the stiffness and coefficient of damping for calculating contact force. In this model, solid-to-solid type contact is provided between the contacting surfaces, which uses the impact method to calculate the contact force. The contact damping and stiffness are calculated using Hertzian contact theory, which states that the contact force varies with penetration depth and mating surfaces. The contact force tangential component is called the dry friction force, which can be calculated by the Coulomb friction model. For every slip velocity, the Adams solver uses four input characteristics: static and dynamic friction coefficients and static and friction transition velocities to calculate the coefficient of friction. These parameters depend on bearing material and types of used lubricant. The product of the normal force and the friction coefficient gives traction force.

As discussed above, an impact function is used in the Adams solver to calculate the contact force between two contacting surfaces; see Figure 3.

$$F = \begin{cases} 0 & if\ x \geq x_1 \\ \max(0, K(x_1 - x)^e - STEP(x, x_1 - d, R, x_1, 0)\dot{x}) & if x < x_1 \end{cases} \tag{19}$$

where x represents the distance, variable used for computing the impact function, $\dot{x}$ specifying the velocity to impact. x_1 specifies the free length of x (if x < x1, then it gives a positive value for the force; else, the force is zero). 'K' specifies the stiffness of the boundary surface interaction. 'e' represents the force exponent. R denotes the maximum damping coefficient. The boundary dispersion at which ADAMS applies full damping is indicated by the letter "d".

Dynamic Modelling of Single Stage Spur Gear Transmission System

The dynamic model of the single-stage spur gear transmission system modelled in ADAMS view is depicted in Figure 4. It consists of two shafts (i.e., pinion and gear), which are mounted on two bearings on both ends of it. These bearings are supported by a spring mass damper in both horizontal and vertical directions using a pedestal. The motion of pinion as well as gear shafts is constrained to rotation about their own axis by defining revolute joints with the ground and supports. The gears are modelled from the tools provided in the Adams view/Machinery. The parameters used to build the gear model are listed in Table. 4.

To transfer motion and torque applied on shafts to gears, a fixed joint is defined between the shaft and the corresponding gear. In this model, contact surfaces between gear teeth are flexible, whereas the shafts and gear are stiff. So, a contact constraint is defined between two gears to determine the contact force. To simulate the developed model, the parameters of the contact constraint are assumed. See Table. 5. The input torque is applied to the pinion, and the resulting output torque is transferred to the gear as a load. The pinion shaft is connected to the connecting shaft, which is powered by a rotor through a belt and pulley system to drive the spur gear system. The pulleys are constrained to corresponding shafts by providing a fixed joint between them.

Table. 3. Parameters used for modelling the rolling contact ball bearing system.

Parameters	**Value**
Damping (Ns/m)	1000
Stiffness (N/m)	1.0×10^7
Friction coefficient (Dynamic) (μ_k)	0.65
Friction coefficient (Static) (μ_s)	0.78
Boundary dispersion (m)	1.0×10^{-5}
Force exponent (e)	2.2

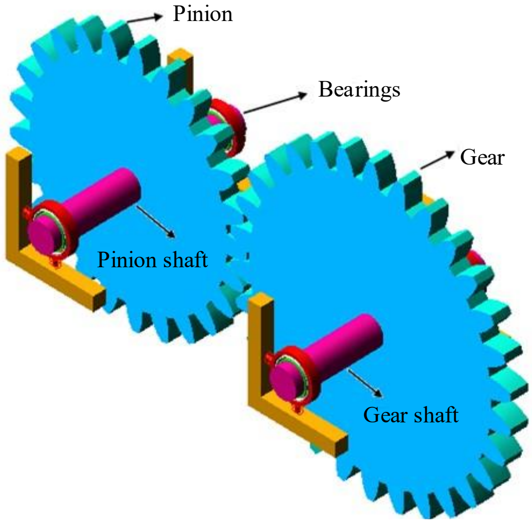

Figure 4. Dynamic model of spur gear pair system.

Table. 4. Parameters used in modelling a single-stage spur gear system.

Parameters	**Gear**	**Pinion**
No. of teeth	30	25
Pressure angle (°)	20	20
Module (mm)	2	2
Width of teeth (cm)	2	2
Mass (gm)	443.9	308.3
Contact ratio	1.63	1.63
Poisson's ratio	0.3	0.3
Young's modulus (N/m^2)	2×10^8	2×10^8
Torque (Nm)	72	60
Rotational speed (rpm)	500	600
Moment of inertia(kgm^2)	2×10^{-4}	0.94×10^{-4}

Table. 5. Parameters used for modelling spur gear system

Parameters	**Value**
Stiffness (N/m)	1.5×10^8
Damping (Ns/m)	67
Force exponent (e)	2.2
Boundary penetration (m)	1.0×10^{-5}
Friction coefficient (Static) (μ_s)	0.78
Friction coefficient (Dynamic) (μ_k)	0.65
Transition velocity (Stiction) (m/s)	1.0
Transition velocity (Friction) (m/s)	100.0

SIMULATION SETUP FOR BALL BEARING SYSTEM AND SPUR GEAR SYSTEM

The developed models are simulated in MSC ADAMS, and the vibration response along the vertical direction of the inner, outer races, and cage (load zone direction) of the ball bearing system and contact force signals along the vertical direction of the spur gear system are collected. The models were simulated under constant speed conditions (600 rpm) for a time window of 10 s with a step size of 0.0001 s. The obtained simulated outcomes were transferred to MATLAB for post-processing because ADAMS doesn't always generate time series data in uphill order or with a consistent sampling interval. Therefore, the data is organized and resampled in MATLAB prior to analysis.

RESULTS AND DISCUSSIONS

Results of Rolling Contact Ball Bearing System

A zoomed portion (0.25 sec time window) of acceleration signals along the vertical direction for the ball, cage, inner and outer races of the ball bearing, and their corresponding frequency response are shown in Figure 5. (a-h). Initially the inner race has rotation, and all other parts are not moving, making the setup transient in initial conditions, which becomes steady after some time. In Figure 5. (b), (d), (f), and (h), we can see that there are very small peaks or no peaks at the characteristic defect frequencies of the bearing parts (BSF, FTF, BSFO, BSPI). This shows that the bearing model is in healthy condition without any defects. Thus, the developed model can be said to be valid.

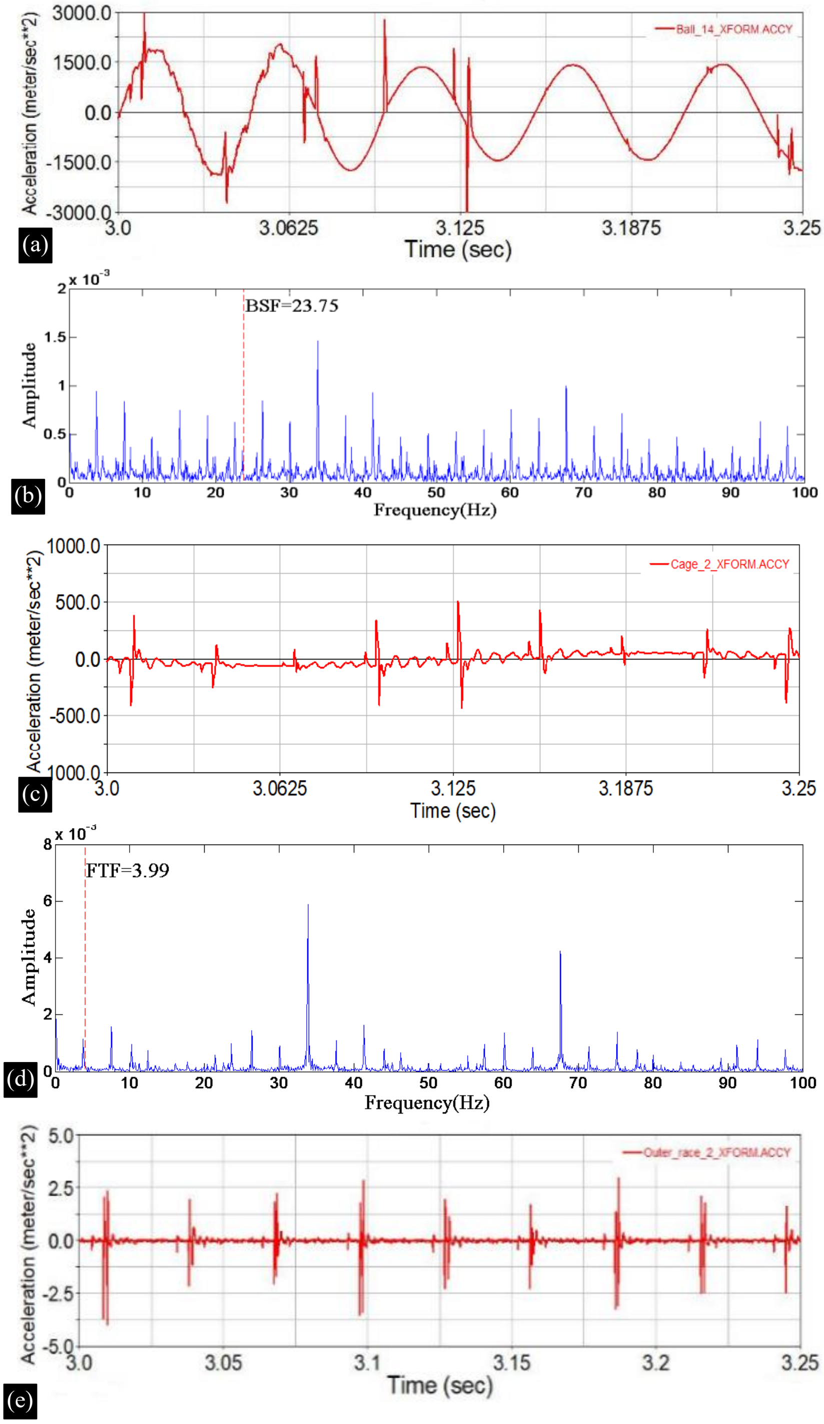

Journal of Polymer & Composites
Volume 13, Special Issue 5
ISSN: 2321-2810 (Online), ISSN: 2321-8525 (Print)

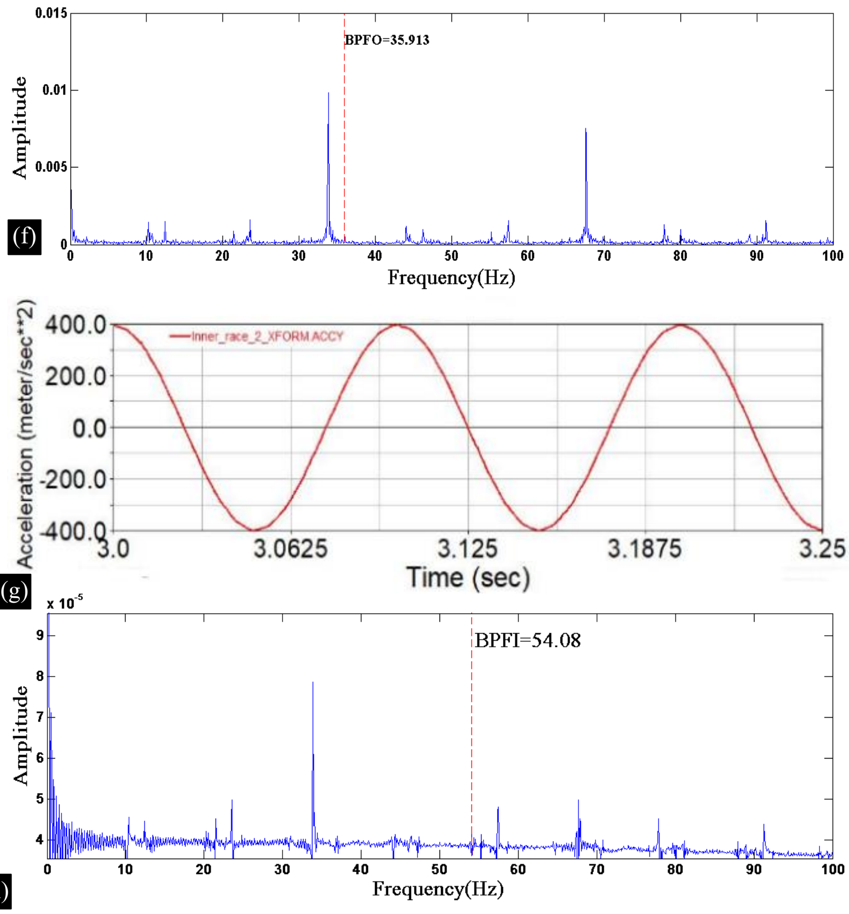

Figure 5. A zoomed portion of acceleration signal along vertical direction and corresponding FFT for (a, b) ball (c, d) cage (e, f) outer race (g, h) inner race of rolling contact ball bearing.

Results of Single Stage Spur Gear System

A zoomed portion (0.1 sec time window) of contact force along the vertical direction and the corresponding frequency domain signal for the pinion and gear of the spur gear model, which is operated under constant speed conditions, is depicted in Fig. 6 (a-d). By observing the obtained frequency domain vibration signal shown in Fig. 6(c), we can say that there will be one peak in the signal for every 250 Hz. which means that for every 1/250 sec, one tooth of the gear will come and leave the contact with other teeth of another gear, which defines the gear meshing frequency of the developed dynamic model. The GMF obtained from the vibration signal seems to fit with the theoretical value. GMF values are always repeated with an integer multiplier known as harmonics. f_m represents the fundamental gear mesh frequency. $2f_m$, $3f_m$, and $4f_m$ represent harmonics of the fundamental frequency.

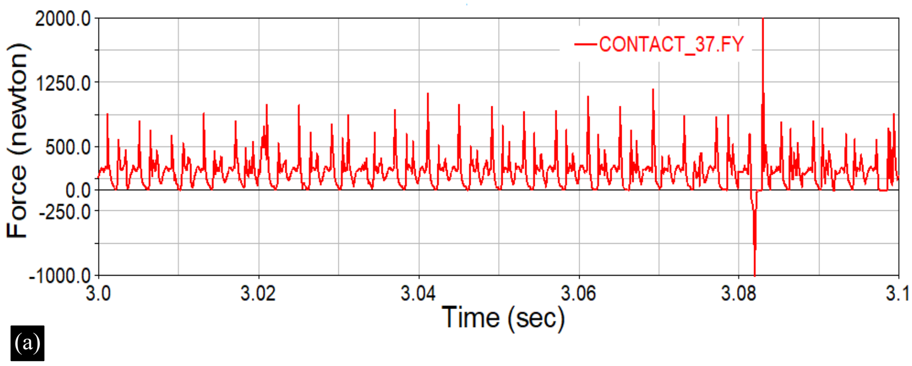

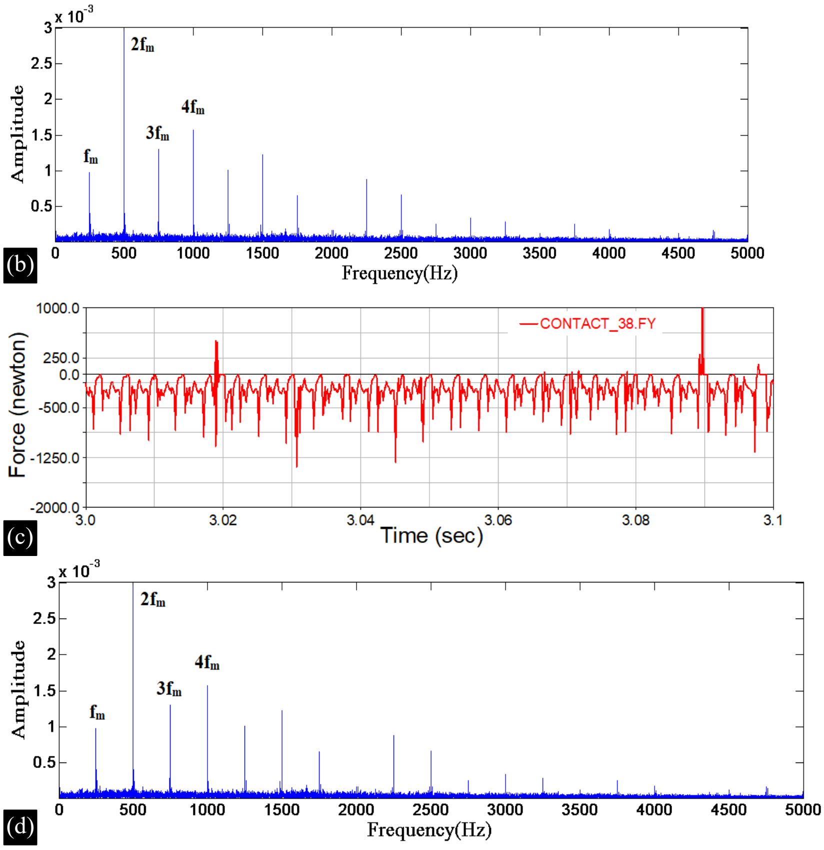

Figure 6. A zoomed portion of contact force along vertical direction and corresponding FFT for (a, b) pinion and (c, d) gear of the spur gear model.

CONCLUSIONS

Dynamic models of rolling contact ball bearing and single-stage spur gear systems are modelled in ADAMS (multi-body dynamic simulation) software. To verify the developed models, they are simulated under constant speed conditions, and acceleration signals of bearing parts and contact force signals of meshing gears are collected. For the obtained vibration signal in the gear system, the corresponding frequency domain signal is generated in MATLAB. As there are very small vibrations or no vibrations at the DCFs of the bearing, and as the GMF value obtained from the frequency domain signal matches with the theoretically calculated value, we can conclude that the developed models are accurate for further analysis.

REFERENCES

1. Daton I., Koren N., Klein R., Bortman J., A realistic dynamic model for gear fault diagnosis. Engineering Failure Analysis. 2018; 84: 77–100p.
2. Sun R., Yang Z., Chen X., Tian S., Xie Y., Gear fault diagnosis based on the structured sparsity time-frequency analysis. Mechanical Systems and Signal Processing. 2018; 102: 346–363p.
3. Tandon, N., Choudhury, A., A review of vibration and acoustic measurement methods for the detection of defects in rolling element bearings. *Tribology international*. 1999; *32*: 469-480p.
4. McFadden P. D., Smith J. D., Model for the vibration produced by a single point defect in a rolling element bearing. Journal of Sound and Vibration. 1984; 96: 69-82p.
5. Mishra C., Samantaray A. K., Chakraborty G., Ball bearing defect models: A study of simulated and experimental fault signatures. Journal of sound and vibration. 2017; 400: 86-112p.
6. Guo, Y., Parker, R. G., Dynamic modeling and analysis of a spur planetary gear involving tooth wedging and bearing clearance nonlinearity. *European Journal of Mechanics-A/Solids*. 2010; *29*: 1022-1033p.

7. Endo H., Randall R. B., Gosselin C., Differential diagnosis of spall vs. cracks in the gear tooth fillet region: Experimental validation. Mechanical Systems and Signal Processing. 2009; 23: 636–651p.
8. Parey A., Badaoui M. E., Guillet F., Tandon N., Dynamic modelling of spur gear pair and application of empirical mode decomposition-based statistical analysis for early detection of localized tooth defect. Journal of Sound and Vibration. 2006; 294: 547–561p.
9. Luo Y., Baddour N., Liang M., Dynamical modelling and experimental validation for tooth pitting and spalling in spur gears. Mechanical Systems and Signal Processing. 2019; 119: 155–181p.
10. Chaari F., Baccar W., Abbes M. S., Haddar M., Effect of spalling or tooth breakage on gear mesh stiffness and dynamic response of a one-stage spur gear transmission. European Journal of Mechanics A/Solids. 2008; 27: 691–705p.
11. Li F., Li R., Tian L., Chen L., Liu J., Data-driven time-frequency analysis method based on variational mode decomposition and its application to gear fault diagnosis in variable working conditions. Mechanical Systems and Signal Processing. 2019; 116: 462-479p.
12. Kumar, R., Mitra, R.K., Dewangan, R., Mishra, C., Modelling and diagnosis of faults in simple bevel gear train. *Wear*. 2023; *524*: 204881p.
13. Kumar, R., Mandal, S., Mishra, C., Hui, N. B., Mitra, R. K., Defect Diagnosis of Bevel Gear System: A Study of Experimental and Simulated Signal. *Journal of Sound and Vibration*. 2024; *593*: 118658p.
14. Kumar, R., Mandal, S., Bhardwaj, P., Mishra, C., Mahato, S., Defect diagnosis of high contact ratio spur gear system with increasing level of fault. *Engineering Failure Analysis*. 2025: *169*: 109097p.
15. Kumar, R., Nanda, P., Mishra, C., Mitra, R. K., December. Modelling, Simulation and Defect Diagnosis of an Epi-cyclic Gear. In *International Conference on Industrial Problems on Machines and Mechanism,* Singapore: Springer Nature Singapore. 2022; 383-392p.
16. Kumar, R., Mishra, C. and Mitra, R.K., December. Modeling and Diagnosis of High Contact Ratio Gear Faults. In *Structural Integrity Conference and Exhibition,* Singapore: Springer Nature Singapore. 2022; 631-645p.
17. Ozguven H. N., Houser D. R., Dynamic analysis of high-speed gears by using loaded static transmission error. Journal of sound and vibration, 1988; 125: 71-83p.
18. Saxena A., Parey A., Chouksey M., Time varying mesh stiffness calculation of spur gear pair considering sliding friction and spalling defects. Engineering Failure Analysis. 2016; 70: 200–211.
19. Yavuz S. D., Saribay Z. B., Cigeroglu E., Nonlinear time-varying dynamic analysis of a spiral bevel geared system. Nonlinear Dynamics. 2018; 92: 1901–1919p.
20. Chen Z., Zhai W., Shao Y., Wang K., Sun G., Analytical model for mesh stiffness calculation of spur gear pair with non-uniformly distributed tooth root crack. Engineering Failure Analysis. 2016; 66: 502–514p.
21. Wang Q., Zhao B., Fu Y., Kong X., Ma H., An improved time-varying mesh stiffness model for helical gear pairs considering axial mesh force component. Mechanical Systems and Signal Processing. 2018; 106: 413–429p.
22. Pandiyarajan R., Starvin M. S., Ganesh K. C., Contact Stress Distribution of Large Diameter Ball Bearing Using Hertzian Elliptical Contact Theory. Procedia Engineering. 2012; 38: 264 – 269.

